Synthesis and Characterization of Nanodiamond–Growth Factor Complexes Toward Applications in Oral Implantation and Regenerative Medicine

Julie Ye Rin Bang, BS[1]
Caleb Ting, BS[1]
Peter Wang, BS[1]
Ted Kim, BS[1]
Kenneth Kezhi Wang, BS[1]
Theodore Kee, MS[1]
Darron Miya, DDS[1]
Dean Ho, PhD[1,2]*
Dong-Keun Lee, PhD[1]*

Introduction

During the past 2 decades, regenerative medicine has emerged as a promising field that is progressing toward tissue regeneration for a broad range of indications.[1,2] However, a current challenge of the field is the need to identify biocompatible and scalable delivery agents to enhance treatment efficacy and safety. Several approaches have attempted to use biomaterials as growth factor carriers for possible sustained delivery and controlled molecular release. For example, incorporation of platelet-derived growth factor into biomaterials (Regranex) has demonstrated successful wound healing and morphogenic proteins 2 and 7 (Infuse, Stryker's OP-1) for bone formation.[3] Additional approaches have sought to improve bone graft treatment outcomes.[4,5] Previous studies on the use of nano-featured titanium surfaces and nanodiamond (ND)–mediated delivery of estrogen in oral implantology demonstrated a stimulation in bone formation, cleft lip palatal expansion, and resistance to chemical corrosion in oral implants.[6–8] In perspective, the application of nanotechnology positively influences oral implantology and improves clinical practice such as osseointegration.

Nanoscale drug delivery vehicles have emerged as a promising strategy for tissue regeneration and controlled release of biomolecules. Many studies of nanoparticle drug delivery platforms have validated the use of nanotechnology for tissue repair.[6–15] Additional studies emphasizing the role of nanoparticle size, shape, charge, and surface chemistry on their resulting toxicity have also been conducted.[16,17] Among the many promising nanoscale drug delivery vehicles that are being explored, NDs have emerged as promising, clinically relevant candidates.[9–15,18] Nanodiamonds are carbon nanoparticles with truncated octahedral structures that are approximately 5 nm in diameter. They are biocompatible products that can be economically processed by ultrasonication, centrifugation, and milling methodologies.[16,19] The surface chemistries of NDs, which are suitable for both electrostatic physisorption and chemical conjugation of a broad spectrum of therapeutics, mediate both high-affinity drug binding and sustained release.[20–40] These characteristics may enable the NDs to serve as translationally relevant growth factor delivery vehicles. In this study, NDs were complexed with epidermal growth factor (EGF) functionalized with Alexa Fluor 488. Epidermal growth factor has previously been explored as a potential agent to promote osteogenic differentiation.[17,41] Therefore, ND-EGF may serve as an agent to enhance osteogenesis. In this study, EGF binding and release studies confirmed that the successful loading of EGF onto the NDs, as well as their prolonged elution, served as an indicator for the prospective applicability of the NDs as drug delivery biomaterials in the field of regenerative medicine.

Materials and Methods

ND-EGF synthesis and characterization

ND-EGF was synthesized by diluting autoclaved ND solution (NanoCarbon Research Institute Co, Ltd, Nagano, Japan) with H_2O (autoclaved). Then, 0.2 mL (20 μg) of EGF streptavidin biotin-modified Alexa Fluor 488 (Thermo Fisher Scientific, Canoga Park, Calif) was added to the solution and mixed,

[1] Division of Oral Biology and Medicine, School of Dentistry, UCLA, Los Angeles, Calif.
[2] Department of Bioengineering, School of Engineering and Applied Science, UCLA, Los Angeles, Calif.
* *Corresponding authors,* e-mails: nanoscientist@ucla.edu and dho@dentistry.ucla.edu
DOI: 10.1563/aaid-joi-D-17-00120

along with 1M NaOH (Sigma-Aldrich, St Louis, Mo) for aggregation of ND-EGF complexes. The resulting solution was incubated for a minimum of 3 days, at a temperature of 22°C, and was protected from any source of light. After centrifugation, the first supernatant sample was collected for further analysis, and the resulting pellet was diluted and centrifuged further. A second supernatant sample was collected and also saved for further analysis, while the pellet was resuspended in H_2O with a probe sonicator to generate a 5-mg/mL ND solution. The EGF complexed with Alexa Fluor 488 was used to conduct 1:1 serial dilutions, which were analyzed to generate a standard curve.

Two supernatants with unknown Alexa 488 concentrations were collected from the synthesis of ND-EGF. Serial dilutions were analyzed using a BioTek Synergy H1 microplate reader (BioTek Instruments, Inc, Winooski, Vt) and Gen5 2.03 computer software for fluorescence spectroscopy at an excitation wavelength of 350 nm and an emission wavelength of 520 nm.[42–45] Using samples of known concentration and resulting fluorescent intensity obtained from light spectroscopy, a linear trend with its respective equation was generated from the data. From this equation, the Alexa 488 concentrations of the 2 supernatant solutions were calculated using the measured intensity of each sample and plotting the measured intensities along the previously generated standard curve, which gave indications of the amount of EGF functionalized onto NDs. Characterization of the ND-EGF by dynamic light scattering (DLS) and ζ-potential analysis was conducted using the Zetasizer Nano ZS (Malvern, Worcestershire, UK).

ND-EGF release profile

Two solutions of biological media were synthesized to provide the ND-EGF compound a simulated biological environment. The first (1:1 biological medium) being a Dulbecco's Modified Eagle Media (DMEM; Thermo Fisher Scientific) and streptomycin (Thermo Fisher Scientific**)** with 10% fetal bovine serum:phosphate-buffered saline (FBS:PBS) mixture in 1:1 ratio (FBS from Gemini Bio Products, West Sacramento, Calif; PBS from Thermo Fisher Scientific). The second solution (1:10 biological medium) was a DMEM and streptomycin with 10% FBS:PBS mixture in 1:10 ratio.[46] A sample containing 5 μg of EGF-conjugated Alexa 488 was taken from the ND-EGF solution and centrifuged for 20 minutes at 14 000*g*. The solution was removed, and 1 mL of biological media was added to the ND-EGF sample for the releasing experiment. Two sets of media were made, with one containing 1:1 and the second containing 1:10 ratios of biological medium with 10% FBS:PBS. The ND-EGF was dispersed within the media, incubated at 36.6°C for 1 hour, and then centrifuged for 20 minutes at 14 000*g*. Supernatant was extracted from both tubes, and the pellet within each tube was gently detached from the bottom. One milliliter of fresh new media was added back into their respective tubes containing ND-EGF. This procedure was repeated every hour for the next 4 hours and then again at hours 18, 30, 50, 100, 170, and 240, each resulting in a new pair of supernatant solutions ready for fluorescent analysis. All supernatant samples were loaded onto a 96-well plate and analyzed for fluorescence at excitation wavelength 350 nm and emission wavelength 520 nm. The ND-EGF solution containing 1:1 biological medium was then diluted to a 1:10 biological medium solution for further fluorescence spectroscopy analysis.

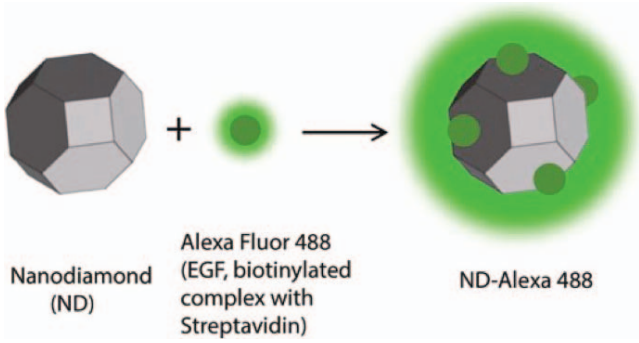

Figure 1. A model of nanodiamonds conjugated with epidermal growth factor complexed to Alexa Fluor 488.

Results

ND-EGF synthesis and characterization

A schematic of ND-EGF is shown in Figure 1. As shown in Figure 2a and b, EGF was readily loaded onto the ND surface, which was also observed after multiple rounds of incubation and centrifugation. This was further demonstrated after the measured fluorescence intensity was compared with the standard curve of background Alexa Fluor 488 fluorescence intensity (Figure 2a). Furthermore, characterization performed through DLS and ζ-potential analysis of the ND-EGF complexes exhibited substantially increased particle diameters compared with those of unmodified NDs, from 46.6 ± 0.17 to 184.3 ± 1.03 nm (Figure 3). Additional analysis revealed decreased ζ-potentials for ND-EGF complexes compared with those of unmodified NDs, from 55.8 ± 0.37 to 41.4 ± 0.89 mV, respectively (Figure 3).

ND-EGF release profile

From the standard curve plotted with 1:10 biological medium as a background (Figure 4a), the cumulative EGF conjugated with Alexa-488 release profiles for ND-EGF samples in 1:1 and 1:10 biological media (DMEM with 10% FBS:PBS) were determined. For both samples, sustained EGF functionalized with Alexa-488 release was observed for 11 days, while relatively higher release was observed during the first 5 hours (Figure 4b). The ND-EGF sample in 1:1 diluted biological medium presented greater total fluorescence release (1.83 ± 0.20 μg) than that of the sample in 1:10 biological medium (0.53 ± 0.05 μg) over the same duration.

Discussion

EGF functionalized with Alexa Fluor 488 was used to quantify the rate of drug release when bound to ND particles. To quantify ND-EGF binding efficiency, fluorescent spectroscopy analysis was performed to determine sufficient binding.[47–50] Furthermore, characterization through DLS and ζ-potential analysis of the formation of ND-EGF complex exhibited

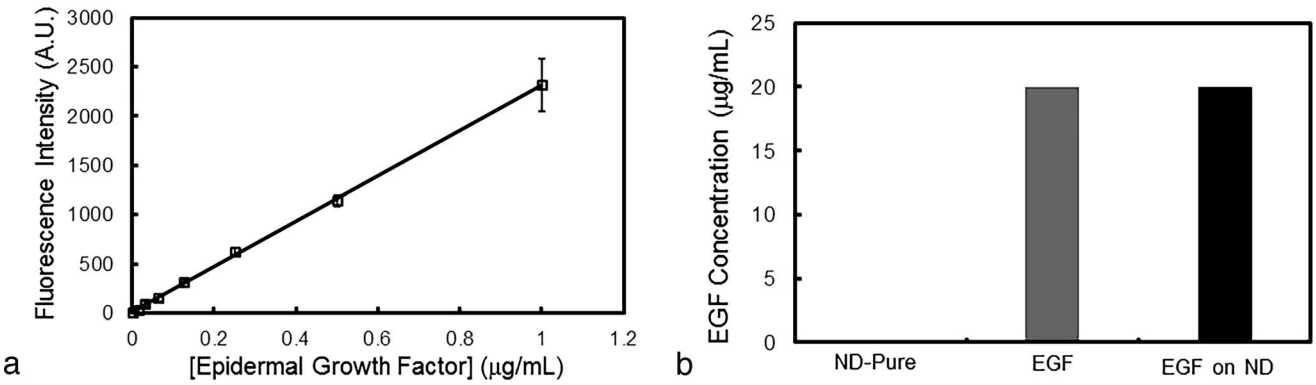

Figure 2. Nanodiamond (ND)–epidermal growth factor (EGF) synthesis and characterization. (a) Standard curve for EGF–Alexa-488 concentrations. (b) The final amount of EGF–Alexa-488 successfully loaded onto ND. Using the standard curve, the loading efficiency for ND-EGF–Alexa-488 was determined. All 20 μg/mL of applied EGF–Alexa-488 was successfully attached to unmodified ND (~100% efficiency) that initially had no fluorescence loaded (0 μg/mL).

substantially increased diameters compared with the diameter of unmodified NDs. However, its relatively small size distribution still makes it a viable method for drug delivery.[45–48] The potential of NDs as a viable drug binding platform is attributed to their unique chemical surface properties, which allow for a variety of electrostatic interactions to occur. Sodium hydroxide (NaOH) was used to induce an electrostatic charge on the surface chemistry of the NDs.[48,51–57] The slight decrease in ζ-potentials in ND-EGF complexes compared with unmodified NDs (Figure 2b) indicates that the ND-EGF complexes are able to form efficient electrostatic interactions with other molecules.

Culture media solution containing various proteins, carbohydrates, and antibiotics was produced with the intention of simulating a physiologically relevant system to test the sustained growth factor release capabilities of NDs. As shown in Figure 4b, the ND-EGF complexes experience sustained drug release in both the 1:1 and the 1:10 biological media over a nearly 2-week-long period. However, the ND-EGF sample within the 1:1 biological medium released larger amounts of EGF over the same period of time compared with when the sample was within the 1:10 biological medium. This can potentially be explained by the higher concentration of proteins within the 1:1 solution compared with the 1:10 solution. Previous studies have demonstrated that charged proteins are able to competitively bind to the surface of NDs, which enhances drug release.[53,54] Similar to EGF, epirubicin chemotherapy drugs, when bound to NDs, displayed an increasing rate of drug release proportional to increases in concentrations of the FBS within the biological media.[58]

Of note, during the EGF release analysis for the 1:1 solution, the concentration of proteins generated a higher than expected intensity background. As a result, the 1:1 ratio solution was diluted to a 1:10 biological medium, resulting in a lower intensity background. Using the diluted solution, the intensity of EGF-Alexa Fluor 488 was measured. Comparing the diluted 1:1 solution with the original 1:10 solution, a consistency in drug release was apparent. After further calculations of the common ratio, the concentrations of EGF–Alexa Fluor 488 released within a 1:1 solution were determined. Data acquired through fluorescent intensity analysis further demonstrated the potential applicability of ND-EGF toward downstream preclinical validation.

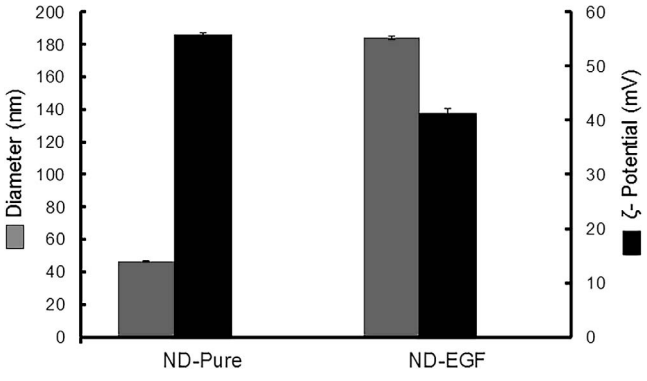

Figure 3. Dynamic light scattering analysis for unmodified nanodiamond (ND) and ND–epidermal growth factor (EGF) samples. The diameters of ND and ND-EGF are 46.6 ± 0.17 nm and 184.3 ± 1.03 nm, and the ζ-potentials of ND and ND-EGF are 55.8 ± 0.37 mV and 41.4 ± 0.89 mV, respectively.

Conclusion

In summary, this work demonstrated the synthesis and characterization of ND-EGF toward potential applications in regenerative medicine. Through fluorescence analysis of the supernatant from each solution, the concentration of the released protein was determined. Sustained EGF elution from the ND complexes was confirmed in physiologically relevant solutions with 2 different ratios of proteins and carbohydrates. Thus, this work confirms the sustained release capabilities of NDs and provides valuable support for the potential applications of NDs to deliver growth factors and other therapeutics in a variety of medical applications.

Abbreviations

DMEM: Dulbecco's Modified Eagle's Medium
EGF: epidermal growth factor
FBS: fetal bovine serum

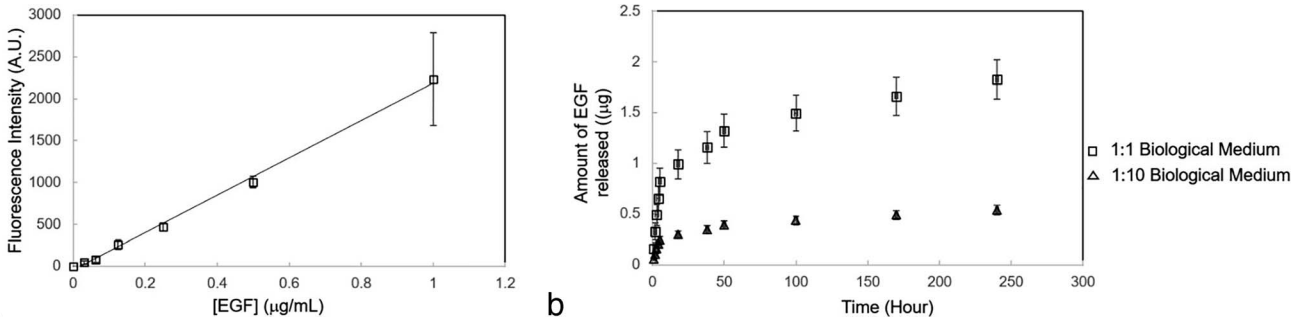

Figure 4. Nanodiamond (ND)–epidermal growth factor (EGF) fluorescence release profile. (a) Standard curve for EGF conjugated to Alexa-488 with 1:10 biological medium (Dulbecco's Modified Eagle Media [DMEM] and streptomycin with 10% fetal bovine serum [FBS]:phosphate-buffered saline [PBS] with water). (b) Cumulative EGF functionalized with Alexa-488 release profiles for ND-EGF samples in 1:10 biological medium and 1:1 biological medium (DMEM and streptomycin with 10% FBS:PBS). For both samples, sustained EGF functionalized with Alexa-488 release was observed for 11 days, with comparatively higher release observed during first 5 hours. The ND-EGF sample in 1:1 biological medium presents greater total fluorescence release (1.83 ± 0.20 μg) than the sample in 1:10 biological medium (0.53 ± 0.05 μg).

ND: nanodiamond

PBS: phosphate-buffered saline

Acknowledgment

The authors gratefully acknowledge the American Academy of Implant Dentistry (AAID) Foundation for the support of this work under award 20150460.

Note

D.H. and D.-K.L. are co-inventors of pending patents pertaining to nanodiamond drug delivery.

References

1. Mao AS, Mooney DJ. Regenerative medicine: current therapies and future directions. *Proc Natl Acad Sci USA*. 2015;112:14452–14459.
2. Terzic A, Pfenning MA, Gores GJ, Harper CM. Regenerative medicine build-out. *Stem Cells Transl Med*. 2015;4:1373–1379.
3. Walsh G. Biopharmaceutical benchmarks 2010. *Nat Biotechnol*. 2010;28:917–924.
4. Papanas N, Maltezos E. Becaplermin gel in the treatment of diabetic neuropathic foot ulcers. *Clin Interv Aging*. 2008;3:233–240.
5. Epstein NE. Basic science and spine literature document bone morphogenetic protein increases cancer risk. *Surg Neurol Int*. 2014;5:552–560.
6. Baena RRY, Rizzo S, Manzo L, Lupi SM. Nanofeatured titanium surfaces for dental implantology: biological effects, biocompatibility, and safety. *J Nanomater*. 2017;2017:1–18.
7. Auciello O, Gurman P, Guglielmotti MB, Olmedo DG, Berra A, Saravia MJ. Biocompatible ultrananocrystalline diamond coatings for implantable medical devices. *MRS Bull*. 2014;39:621–629.
8. Hong C, Song D, Lee D-K, et al. Reducing posttreatment relapse in cleft lip palatal expansion using an injectable estrogen–nanodiamond hydrogel. *Proc Natl Acad Sci USA*. 2017;114:E7218–E7225.
9. Engel E, Michiardi A, Navarro M, Lacroix D, Planell JA. Nanotechnology in regenerative medicine: the materials side. *Trends Biotechnol*. 2008;26:39–47.
10. Perán M, García MA, López-Ruiz E, et al. Functionalized nanostructures with application in regenerative medicine. *Int J Mol Sci*. 2012;13:3847–3886.
11. Gobin AM, Lee MH, Halas NJ, James WD, Drezek RA, West JL. Near-infrared resonant nanoshells for combined optical imaging and photothermal cancer therapy. *Nano Lett*. 2007;7:1929–1934.
12. Hom C, Lu J, Liong M, Luo H, Li Z, Zink JI, Tamanoi F. Mesoporous silica nanoparticles facilitate delivery of siRNA to shutdown signaling pathways in mammalian cells. *Small*. 2010;6:1185–1190.
13. Deming TJ. Methodologies for preparation of synthetic block copolypeptides: materials with future promise in drug delivery. *Adv Drug Deliv Rev*. 2002;54:1145–1155.
14. Peer D, Karp JM, Hong S, Farokhzad OC, Margalit R, Langer R. Nanocarriers as an emerging platform for cancer therapy. *Nat Nanotechnol*. 2007;2:751–760.
15. Liu Z, Robinson JT, Sun X, Dai H. PEGylated nanographene oxide for delivery of water-insoluble cancer drugs. *J Am Chem Soc*. 2008;130:10876–10877.
16. Davis ME, Zuckerman E, Choi CH, et al. Evidence of RNAi in humans from systemically administered siRNA via targeted nanoparticles. *Nature*. 2010;464:1067–1070.
17. Zhang Q, Mochalin VN, Neitzel I, et al. Fluorescent PLLA-nanodiamond composites for bone tissue engineering. *Biomaterials*. 2011;32:87–94.
18. Kostarelos K, Lacerda L, Pastorin G, et al. Cellular uptake of functionalized carbon nanotubes is independent of functional group and cell type. *Nat Nanotechnol*. 2007;2:108–113.
19. Aillon KL, Xie Y, El-Gendy N, Berkland CJ, Forrest ML. Effects of nanomaterial physicochemical properties on in vivo toxicity. *Adv Drug Deliv Rev*. 2009;61:457–466.
20. Kruger A, Kataoka F, Ozawa M, et al. Unusually tight aggregation in detonation nanodiamond: identification and disintegration. *Carbon*. 2005;43:1722–1730.
21. Huang H, Pierstorff E, Osawa E, Ho D. Active nanodiamond hydrogels for chemotherapeutic delivery. *Nano Lett*. 2007;7:3305–3314.
22. Barnard AS. Self-assembly in nanodiamond agglutinates. *J Mater Chem*. 2008;18:4038–4041.
23. Barnard AS. Diamond standard in diagnostics: nanodiamond biolabels make their mark. *Analyst*. 2009;134:1751–1764.
24. Adnan A, Lam R, Chen H, et al. Atomistic simulation and measurement of pH dependent cancer therapeutic interactions with nanodiamond carrier. *Mol Pharm*. 2011;9:368–374.
25. Tisler J, Balasubramanian G, Naydenov B, et al. Fluorescence and spin properties of defects in single digit nanodiamonds. *ACS Nano*. 2009;3:1959–1965.
26. McGuinness LP, Yan Y, Stacey A, et al. Quantum measurement and orientation tracking of fluorescent nanodiamonds inside living cells. *Nat Nanotechnol*. 2011;6:358–363.
27. Liang Y, Ozawa M, Krueger A. A general procedure to functionalize agglomerating nanoparticles demonstrated on nanodiamond. *ACS Nano*. 2009;3:2288–2296.
28. Heyer S, Janssen W, Turner S, et al. Toward deep blue nano dope diamonds: heavily boron-doped diamond nanoparticles. *ACS Nano*. 2014;8:5757–5764.

29. Mohan N, Chen CS, Hsieh HH, Wu YC, Chang HC. In vivo imaging and toxicity assessments of fluorescent nanodiamonds in *Caenorhabditis elegans*. *Nano Lett*. 2010;10:3692–3699.

30. Hui YY, Cheng CL, Chang HC. Nanodiamonds for optical bioimaging. *J Phys D Appl Phys*. 2010;43:374021.

31. Wu TJ, Tzeng VK, Chang WW, et al. Tracking the engraftment of regenerative capabilities of transplanted lung stem cells using fluorescent nanodiamonds. *Nat Nanotechnol*. 2013;3:682–689.

32. Hui YY, Su LJ, Chen OY, Chen YT, Liu TM, Chang HC. Wide-field imaging and flow cytometric analysis of cancer cells in blood by fluorescent nanodiamond labeling and time gating. *Sci Rep*. 2014;4:5574.

33. Liu KK, Wang CC, Cheng CL, Chao JI. Endocytic carboxylated nanodiamond for the labeling and tracking of cell division and differentiation in cancer and stem cells. *Biomaterials*. 2009;30:4249–4259.

34. Liu KK, Zeng WW, Wang CC, et al. Covalent linkage of nanodiamond-paclitaxel for drug delivery and cancer therapy. *Nanotechnology*. 2010;21:315106.

35. Perevedentseva E, Lin Y, Jani M, Cheng CL. Biomedical applications of nanodiamonds in imaging and therapy. *Nanomedicine*. 2013;8:2041–2060.

36. Huang H, Pierstorff E, Osawa E, Ho D. Protein-mediated assembly of nanodiamond hydrogels into a biocompatible and biofunctional multilayer nanofilm. *ACS Nano*. 2008;2:203–212.

37. Kumar A, Lin PA, Xue A, Hao B, Yap YK, Sankaran RM. Formation of nanodiamonds at near-ambient conditions via microplasma dissociation of ethanol vapour. *Nat Commun*. 2013;4:2618.

38. Xing Z, Pedersen TP, Wu X, et al. Biological effects of functionalizing copolymer scaffolds with nanodiamond particles. *Tissue Eng Part A*. 2013;19:1783–1791.

39. Havlik J, Petrakova V, Rehor I, et al. Boosting nanodiamond fluorescence: towards development of brighter probes. *Nanoscale*. 2013;10:3728–3735.

40. Mochalin VN, Pentecost A, Li XM, et al. Absorption of drugs on nanodiamond: toward development of a drug delivery platform. *Mol Pharm*. 2013;10:3728–3735.

41. Mochalin V, Shenderova O, Ho D, Gogotsi Y. The properties and applications of nanodiamonds. *Nat Nanotechnol*. 2012;7:11–23.

42. Marquez L, de Abreu FA, Ferreira CL, Alves GD, Miziara MN, Alves JB. Enhanced bone healing of rat tooth sockets after administration of epidermal growth factor (EGF) carried by liposome. *Injury*. 2013;44:558–564.

43. Del Angel-Mosqueda C, Gutiérrez-Puente Y, López-Lozano AP, et al. Epidermal growth factor enhances osteogenic differentiation of dental pulp stem cells in vitro. *Head Face Med*. 2015;11:29.

44. Chao JI, Perevedentseva E, Chung PH, et al. Nanometer-sized diamond particle as a probe for biolabeling. *Biophys J*. 2007;93:2199–2208.

45. Faklaris O, Joshi V, Irinopoulou T, et al. Photoluminescent diamond nanoparticles for cell labeling: study of the uptake mechanism in mammalian cells. *ACS Nano*. 2009;3:3955–3962.

46. Durkin AJ, Bloomston P, Rosemurgy AS, et al. Defining the role of the epidermal growth factor receptor in pancreatic cancer grown in vitro. *Am J Surg*. 2003;186:431–436.

47. Chow EK, Zhang X-Q, Chen M, et al. Nanodiamond therapeutic delivery agents mediate enhanced chemoresistant tumor treatment. *Sci Transl Med*. 2011;3:73ra21.

48. Hui YY, Cheng CL, Chang HC. Nanodiamonds for optical bioimaging. *J Phys D Appl Phys*. 2010;43:374021.

49. Mochalin VN, Gogotsi Y. Wet chemistry route to hydrophobic blue fluorescent nanodiamond. *J Am Chem Soc*. 2009;131:4594–4595.

50. Chen M, Pierstorff ED, Lam R, et al. Nanodiamond-mediated delivery of water-insoluble therapeutics. *ACS Nano*. 2009;3:2016–2022.

51. Kim HJ, Zhang K, Moore L, Ho D. Diamond nanogel embedded contact lenses mediate lysozyme-dependent therapeutic release. *ACS Nano* 2014;8:2998–3005.

52. Moore L, Chow EKH, Osawa E, Bishop JM, Ho D. Diamond-lipid hybrids enhance chemotherapeutic tolerance and mediate tumor regression. *Adv Mater*. 2013;25:3532–3541.

53. Barnard AS, Sternberg M. Crystallinity and surface electrostatics of diamond nanocrystals. *J Mater Chem*. 2007;17:4811–4819.

54. Barnard AS, Osawa E. The impact of structural polydispersity on the surface electrostatic potential of nanodiamond. *Nanoscale*. 2014;6:1188–1194.

55. Moore L, Gatica M, Kim H, Osawa E, Ho D. Multi-protein delivery by nanodiamonds promotes bone formation. *J Dent Res*. 2013;92:976–981.

56. Chang LY, Osawa E, Barnard AS. Confirmation of the electrostatic self-assembly of nanodiamonds. *Nanoscale*. 2011;3:958–962.

57. Neugart F, Zappe A, Jelezko F, et al. Dynamics of diamond nanoparticles in solution and cells. *Nano Lett*. 2007;7:3588–3591.

58. Wang X, Low XC, Hou W, et al. Epirubicin-adsorbed nanodiamonds kill chemoresistant hepatic cancer stem cells. *ACS Nano*. 2014;8:12151–12166.